Chemical Engineering Journal 165 (2010) 413–419

Contents lists available at ScienceDirect

Chemical Engineering Journal

journal homepage: www.elsevier.com/locate/cej

Desalination based on humidification–dehumidification by air bubbles passing through brackish water

S.A. El-Agouz*

Mechanical Power Engineering Department, Faculty of Engineering, Tanta University, Tanta, Egypt

ARTICLE INFO

Article history:
Received 8 May 2010
Received in revised form 3 September 2010
Accepted 6 September 2010

Keywords:
Air humidification and dehumidification process
Desalination system
Energy conservation

ABSTRACT

Experimental work investigates the principal operating parameters of a proposed desalination process working with an air humidification–dehumidification method. The main objective of this work was to determine the humid air behavior through single stage of desalination system. The experimental work studied the influence of the operating conditions such as the water temperature, the brackish water level and the airflow rate on the desalination performance. The experimental results show that the productivity of the system increases with the increase of the brackish water temperature and the decrease of the airflow rate. The productivity of the system is moderately affected by the brackish water temperature, airflow rate and slightly affected by the brackish water level. The humidification effectiveness and the efficiency of the desalination system are higher for $\dot{m}_a = 14$ kg/h at different brackish water temperatures and levels. Within the studied ranges, the maximum productivity of the system reached to 8.22 kg_w/h at 86 °C for brackish water and $\dot{m}_a = 14$ kg/h. A good agreement was achieved with productivity calculations.

1. Introduction

Humidification–dehumidification desalination (HDH) process is viewed as a promising technique for small capacity production plants. The process has several attractive features, which include operation at low temperature, ability to combine with sustainable energy sources, i.e., solar, geothermal, and requirements of low level of technical features. The humidification–dehumidification process is an interesting technique, which has been adapted for water desalination, where air is used as a carrier gas to evaporate water from the saline feed and to form fresh water by subsequent condensation. The HDH process functions at atmospheric pressure so the components are not submitted to mechanical solicitations. The only characteristic required is the resistance to corrosion. Water desalination by humidification and dehumidification has been the subject of many investigations. Different experimental data are available for using HDH at the pilot or industrial scale. An inspection of these data allows establishing many perspectives for this process.

Careful review of previous literature studies shows that a major part of these studies has focused on the performance evaluation of the HDH system combined with solar energy [1–4]. These studies discussed ways to enhance the distillate production and then maximize the performance of such systems. They inferred that water production depends strongly on the hot water temperature, airflow rate and cooling brackish water temperature. In an attempt to improve the daily productivity of the solar desalination, some studies have developed the multi-stage humidification solar desalination technique [4–8]. This technique consists of several steps of air heating and humidification and leads to high vapor concentration in the airflow. The study reported the vapor content difference in air was approximately 110 g_w/kg_a at 60 °C [4], 138 g_w/kg_a at 60 °C [6], and 138 g_w/kg_a at 60 °C [7] after the 8th, 15th, 4th heating humidifying stages respectively. In addition, mathematical modeling and computer simulation studies of solar desalination units are based on the humidification–dehumidification process [9–14]. These studies focused on studying and analyzing the effects and performance of various components involved in the process. Vlachogiannis et al. [15] have presented a novel concept that includes air humidification followed by mechanical compression. This configuration is reported to have very large specific power consumption, which is almost 100 times greater than that consumed by the conventional mechanical vapor compression process by Ettouney et al. [16]. Dai and Zhang [17] utilized structured packing in the humidification unit. They have reported that the thermal efficiency and water production increase with the increase of inlet water mass flow rate into humidifier. Productivity was achieved around 6.2 kg/m^2/day. Garg et al. [18] studied the experimental design and computer simulation model of a multi-effect humidification/dehumidification (MEH) solar desalination system.

* Fax: +20 506810503.
E-mail address: elagouz2002@yahoo.com.

1385-8947/$ – see front matter © 2010 Elsevier B.V. All rights reserved.
doi:10.1016/j.cej.2010.09.008

Nomenclature

$\dot{m}$	productivity of system (kg/h)
C_p	specific heat of water (kJ/kg K)
h	enthalpy (kJ/kg)
i	interest per year
L	latent heat (kJ/kg)
n	number of life years
P	present capital cost of desalination system
Q	power (W)
T	temperature (°C)

Greek symbols

ω	absolute humidity ($kg_w/kg_{dry\ a}$)
$\Delta\omega$	vapor content difference ($kg_w/kg_{dry\ a}$)
η_d	efficiency of the desalination system (%)
η_h	humidifier efficiency (%)

Subscripts

a	air
cal	calculated
ev	evaporator chamber
in	inlet
m	measured
out	outlet
sat	saturation
vap	vaporization
w	water
Cond	condenser

They found that the increases of hot brackish water temperature at the inlet of the humidifier increase the vapor content difference in the air. Recently, El-Agouz and Abugderah [19] presented an experimental investigation of humidification process by air passing through seawater. They have concluded the maximum vapor content difference of the air about 222 g_w/kg_a at 75 °C for water and air. In addition, the vapor content is high compared to that obtained from single stage and similar to that obtained from multi-stage.

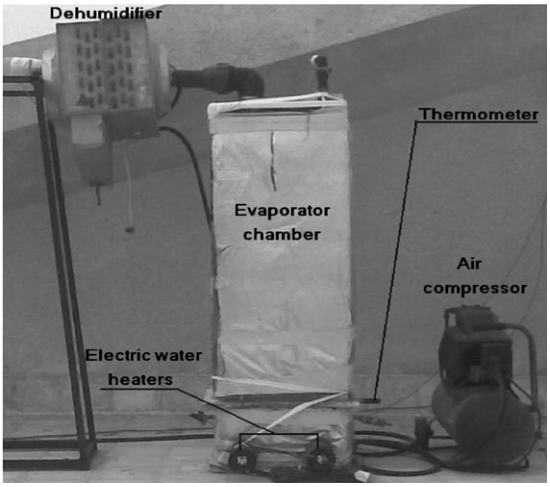

Fig. 2. Photograph of the experimental setup.

It is inferred from the literature that most of the previous works have used heated water spray during the humidification process. In addition, they have used a single system, which produces low water capacity. Therefore, the multi-stage system is used to increase the distillate production. The main objective of this work is the experimental and theoretical investigation of the principal operating parameters of a new desalination process working with an air humidification–dehumidification method. The experimental work studied the influence of the operating conditions such as the brackish water temperature, the seawater level and the airflow rate to evaporator chamber on the desalination performance.

2. Experimental setup and procedure

2.1. Experimental setup

Fig. 1 illustrates a schematic diagram and Fig. 2 shows a photograph of the experimental setup. The system's main components are air compressor (1), evaporator chamber (5) and dehumidifier (12). The desalination system consists of two loops, one for cold brackish water and the other for air. In the water loop, the cold

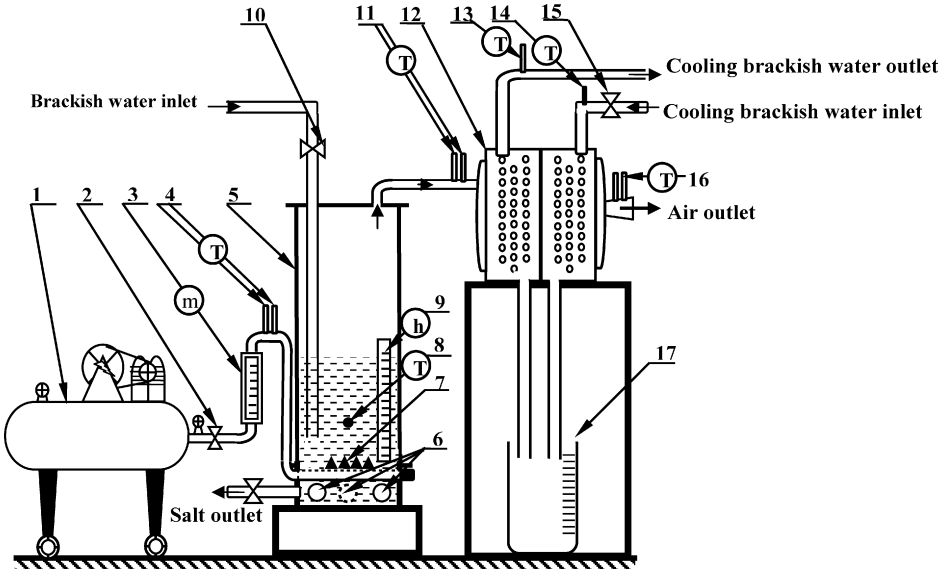

Fig. 1. Schematic diagram of the experimental setup: (1) air compressor, (2) flow control valve, (3) air flow meter, (4, 11, 13, 14, 16) digital thermometer, (5) evaporator chamber, (6) electric water heaters, (7) 44 holes, (8) thermometer PT-100, (9) graduate level, (10,15) flow control valve, (12) dehumidifier, (17) desalinated water tank.

brackish water for evaporator chamber (5) and dehumidifier (12) is supplied from an external source. The water level in the evaporator chamber is controlled by external graduate level (9) and three electric heaters (6) of 1.2 kW power each heat the water. The water level in evaporator chamber is maintained constant and is regulated by a control valve (10). The cold water passes through inner tube of the dehumidifier and is regulated by a control valve (15). *In the air loop*, air for the evaporator chamber (5) is taken from the air compressor discharge, is regulated by a control valve (2), and then is passed through flow meter (3). The airflow enters into the evaporator chamber from 44 holes (7) of 15 mm diameter located at top side of the copper pipe, which is submerged into the water of the evaporator chamber. The air flows through water level in evaporator chamber and carries the vapor water to dehumidifier (12). Then, the produce water through a tube is desalinated to water tank (17). The detailed descriptions of the system's main components are as follows.

2.1.1. Compressor

It consists of two pistons, electrical engine with performance of 3 hp (2.21 kW) work by alternating current AC, compressed air tank with capacity of 200 l. Pressure valve controls the air pressure in the tank, the outlet from the compressor and the outflow rate. Additionally there are some other important devices for controlling the operation of the compressor.

2.1.2. Evaporator chamber

The evaporator chamber (5) consists of lower and upper parts. *The lower part* is made of steel sheet of 1 mm thickness with 400 mm × 300 mm cross section and 250 mm height. It is insulated by glass wool layer insulation with thickness 20 mm, the thermal conductivity is 0.036 W/m K. There are three electric heaters installed in it and 44 holes (7) located at top side of the copper pipe as shown in Fig. 2. *The upper part* is made of thermal glass of 10 mm thickness with 400 mm × 300 mm cross section and 1000 mm height. It is covered by the insulation of polyurethane foam layer with a thickness of 10 mm, the thermal conductivity is 0.023 W/m K and glass wool layer insulation with a thickness of 20 mm, the thermal conductivity is 0.036 W/m K. The glass box is closed by sheet metals of steel of 3 mm thickness that has a hole to exit humid air from humidifier. This hole is connected with a PVC pipe of 75 mm diameter that connects the humidifier with dehumidifier.

2.1.3. Dehumidifier

A two shell and tube heat exchangers connected respectively is used as a dehumidifier. The condensed, freshly produced water is directed through tube to the desalinated water tank. The cooling water flows inside the tubes and the total number of passes is 30 for every heat exchanger. The tubes are made of copper of 9.525 mm diameter. The extended surface is made of 1 mm thick aluminum sheet. The total surface area of every heat exchanger is 4.6 m^2.

2.2. Experimental procedure

The experimental runs are carried out considering the following procedure:

- The temperatures of the system are measured before heating to ensure a uniform temperature of the system.
- The temperature of the water in evaporator chamber is adjusted to the desired temperatures.
- The flow rates of the air stream and the water level in evaporator chamber are adjusted to the desired conditions.

Table 1
The composition of the brackish water.

Composition	mg/l
Ca^{2+}	125
Mg^{2+}	177
$Na^{+} + K^{+}$	785
HCO_3^{-}	345
SO_4^{2-}	535
Cl^{-}	1196
Salinity 3260 mg/l	

- The system is left to reach steady state conditions. The unit is operated at the set conditions for a period of 1.5 h.
- During this period, the control valves with the flow rates of the air and water are continuously monitored and adjusted to the desired flow.
- The desalination system is operated at the set conditions for a period of 1.5 h. During this period, the values of productivity, airflow rate, water level, water temperature, air dry-bulb/wet-bulb temperatures at inlet and outlet evaporator chamber and outlet dehumidifier are recorded at intervals of 5 min and their mean values are calculated.
- Experimental measurements are performed for a new set of conditions.

3. Data acquisition system

Computer-Aided Thermodynamic (Psychometrics) [20] calculates the absolute humidity and enthalpy of the humid air at different points using the dry-bulb/wet-bulb temperatures. The bulb of the wet bulb thermometer is covered with a cotton wick that is saturated with water. Properties of brackish water in experimental is 3530 μs/cm^3 for the conductivity and total dissolved solids (TDS) is 3260 mg/l and Table 1 shows the composition of the brackish water.

The vapor content difference in evaporator chamber is defined as:

$$\Delta\omega_{ev} = \omega_{out} - \omega_{in} \tag{1}$$

The ratio of actual to maximum vapor content difference in evaporator chamber is defined as the humidifier efficiency and is given by:

$$\eta_h = 100 \times \frac{\omega_{out} - \omega_{in}}{\omega_{out,sat} - \omega_{in}} \tag{2}$$

where ω_{out} is outlet absolute humidity; ω_{in} is inlet absolute humidity; and $\omega_{out,sat}$ is outlet absolute humidity at saturation.

The heat rate to the evaporator chamber is defined as:

$$\dot{Q}_{in} = \dot{m}_a \left[(h_{a,out} - h_{a,in}) + \Delta\omega_{ev} C_{p,w}(T_{w,ev} - T_{w,in})\right] \tag{3}$$

where $h_{a,in}$, $h_{a,out}$, $T_{w,ev}$ and $T_{w,in}$, are the inlet humid air enthalpy of the evaporator chamber, the outlet humid air enthalpy of the evaporator chamber, the water temperature in evaporator chamber and the temperature of water inlet evaporator chamber as makeup respectively. The specific heat of the brackish water, $C_{p,w}$ is calculated from [21] as function of salinity.

The thermal efficiency of the desalination system is given by:

$$\eta_d = 100 \times \frac{\dot{m}_{w,m} L_{w,vap}}{\dot{Q}_{in} + \dot{W}_c} \tag{4}$$

where $\dot{m}_{w,m}$ is the water measurement productivity of system; $L_{w,vap}$ is the latent heat of vaporization of water at brackish water temperature in evaporator chamber; $\dot{W}_c$ is the power of compressor.

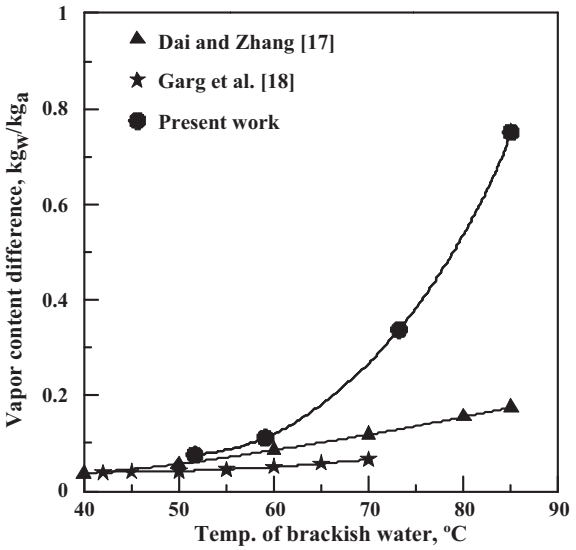

Fig. 3. The comparisons between the present results and those of the, Dai and Zhang [17] and Garg et al. [18].

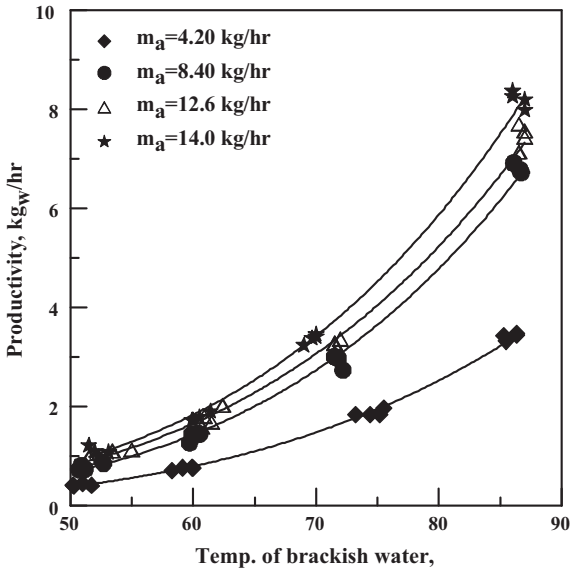

Fig. 4. The effect of the brackish water temperature on the productivity at different airflow rates.

4. Measurement device

As shown in Fig. 1, the air mass flow rate is measured using flow meter in a range from 0 to 18 kg/h with accuracy of ±0.05 g/s. The temperature values of the water, dry-bulb and wet-bulb air at different points of the system (14, 13, 4, 11 and 16) are measured using platinum resistance thermometers. The platinum connected to a digital reading and controller microcomputer thermometer type (Hi9040) in ranging from −50 to 150 °C with accuracy of ±0.1 °C. The voltage and current of the electric water heaters (6) are measured using digital clamp meter type (KSR-266) with accuracy of ±0.1 V and Ampere. The water level head is measured using graduate level with accuracy of ±1 mm. The desalinated water is measured using graduate tank in a range from 0 to 15 l with accuracy of ±0.05 l. To estimate the uncertainties in the results presented in this work, the approach described by Barford [22] was applied. The uncertainty in the measurements is defined as the root sum square of the fixed error of the instrumentation and the random error observed during different measurements. Accordingly, the resulting errors are ±2.74%, ±1.67%, ±1.014% and ±0.3% in the calculated vapor content difference, humidifier efficiency, the power input to the evaporator chamber and the efficiency of the desalination system.

5. A comparison of data with literature

Refs. [17,18] study the same main objective of desalination process working with an air humidification–dehumidification method using different models by spraying water during the humidification process. Therefore, the present experimental results are verified by comparing the obtained results with other published experimental results by [17,18]. Fig. 3 shows that the behavior agreement is good between [17] and [18] and the present results are under the same operating water temperature. The present results show that the vapor content difference in evaporator chamber ($\Delta\omega_{ev}$) is approximately 0.27 kg_w/kg_a at 70 °C and 0.75 g_w/kg_a at 85 °C. The results showed that the vapor content difference in evaporator chamber ($\Delta\omega_{ev}$) is approximately 0.1745 kg_w/kg_a at 85 °C by [17], and the vapor content difference in evaporator chamber ($\Delta\omega_{ev}$) is approximately 0.066 kg_w/kg_a at 70 °C by [18]. Thus, the vapor content difference in evaporator chamber ($\Delta\omega_{ev}$) for the present results is increased around 4.3 and 4.1 times than [17,18] results. In addition, more details for this model are presented, as in [19].

6. Results and discussion

The effect of water temperature and level increase in the evaporator chamber on the productivity of the system is shown in Fig. 4. It is evident from the figures at constant airflow rate that as the temperature increases, the productivity is increased. On the other hand, the productivity is slightly affected by the water level. In addition, as the inlet airflow rate increases, the productivity is increased. This increase in the system output is due to the decrease difference between the air dry-bulb/wet-bulb temperatures. The bubble radius increases to account for the larger flow rate. The mean radius of the bubble produced can be modeled as an exponential function of the gas flow rate, $R \approx (\dot{m}_a)^n$ where R is the radius, $\dot{m}_a$ is the airflow rate, and n, the exponent, ranges from 0.1 to 0.44. Therefore, the increase of airflow rate increases the bubble rise velocity and bubble size. In addition, the increase of the number of air bubbles increases the rate of interface area, which increase the productivity. At 86 °C of the brackish water in evaporator chamber, the average productivity of the system is 3.41, 6.8, 7.45 and 8.22 kg/h at 4.2, 8.4, 12.6 and 14 kg_a/h, respectively.

The effect of water level and airflow rate increase in the evaporator chamber on the productivity of the system at T_w = 50, 60, 70 and 80 °C is shown in Fig. 5. It is evident from the figure that as the level of the water increases, the productivity is slightly increased at all water temperatures. On the other hand, as the airflow rate increases, the productivity is increased at T_w = 60, 70 and 80 °C except for T_w = 50 °C is decreased. This is due to the increase in the diameter and the density distribution and kinetic energy of air bubbles in hot water layer.

Fig. 6 shows the relationship between the humidification efficiency and the temperatures of water at different airflow rates and water levels. As shown in the figures, the humidification efficiency increases with the increase of water temperature and airflow rate at same water level. On other hand, the humidification efficiency is slightly affected with the increase of water temperature and water level at the same airflow rate. The humidification efficiency is higher for $\dot{m}_a$ = 14 kg/h at different water levels and temperatures. The increasing of water temperature and airflow rate for considers ranges increases of average humidification efficiency of the desali-

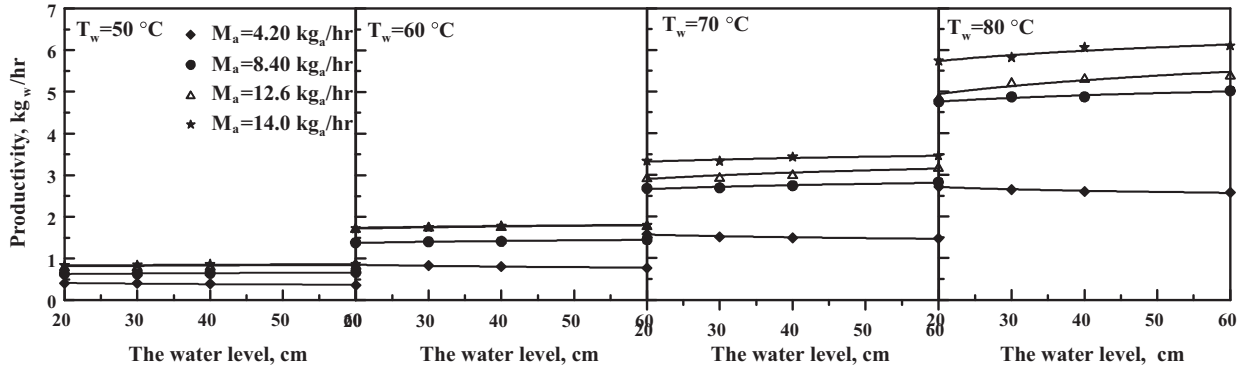

Fig. 5. The effect of the brackish water level on the productivity at different airflow rates and brackish water temperatures.

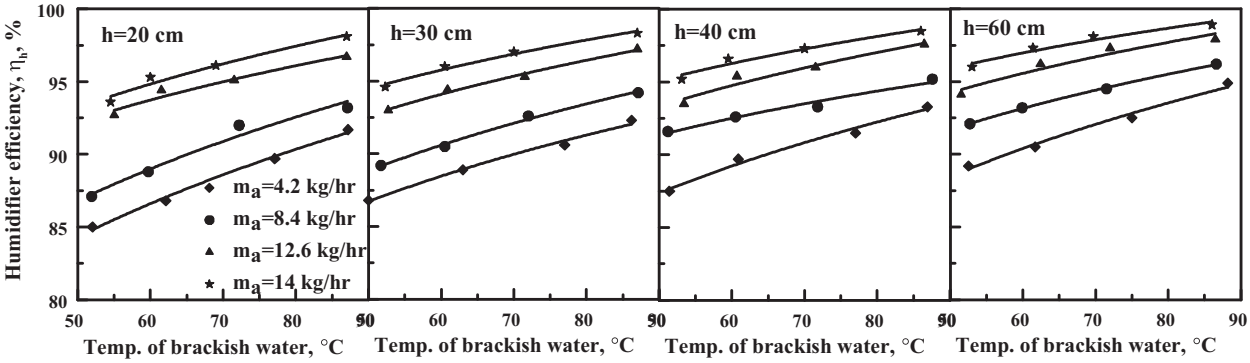

Fig. 6. The effect of the brackish water temperature on the humidification efficiency at different airflow rates and brackish water levels.

nation system is 6.8, 5.3, 4.3 and 3.8% at h = 20, 30, 40 and 60 cm respectively.

Fig. 7 presents the effect of the water temperature at different water levels and airflow rates on the efficiency of the desalination system. As can be seen from Fig. 7, the increase in water temperature and airflow rate increases the efficiency. The efficiency is higher for $\dot{m}_a = 14$ kg/h at different water levels and temperatures. The increasing of water temperature and airflow rate for considers ranges increases of average efficiency of the desalination system is 4.2, 4.3, 4.13 and 3.9% at h = 20, 30, 40 and 60 cm respectively.

7. The comparison between experimental measured and experimental calculated productivity

The comparison between the experimental productivity measurement $(\dot{m}_w)_m$ and calculation $(\dot{m}_w)_{cal}$ is evaluated. The $(\dot{m}_w)_m$ which is collected in water tank (17). The water productivity at the dehumidifier $(\dot{m}_w)_{cal}$ can be calculated by the following equation:

$$(\dot{m}_w)_{cal} = \dot{m}_a(\omega_{in,de} - \omega_{out,de})$$

where $\omega_{in,de}$ and $\omega_{out,de}$ are inlet and outlet absolute humidity for dehumidifier.

The approximated agreement between the experimental productivity calculation and measurement results is good. The shift between the productivity calculation and measurement results is about average 7.7%, 8.5%, 9.94% and 4.5% at airflow rate 4.2, 8.4, 12.6 and 14 kg/h. Because of the experimental productivity calculation correlation is deduced under the steady state condition, the change of surrounding conditions, losses in system, and error in measurement. The decreases between the experimental productivity measurement and calculation due to the increase of mass of air which increase the air velocity and decrease the vapor condensations in evaporator chamber.

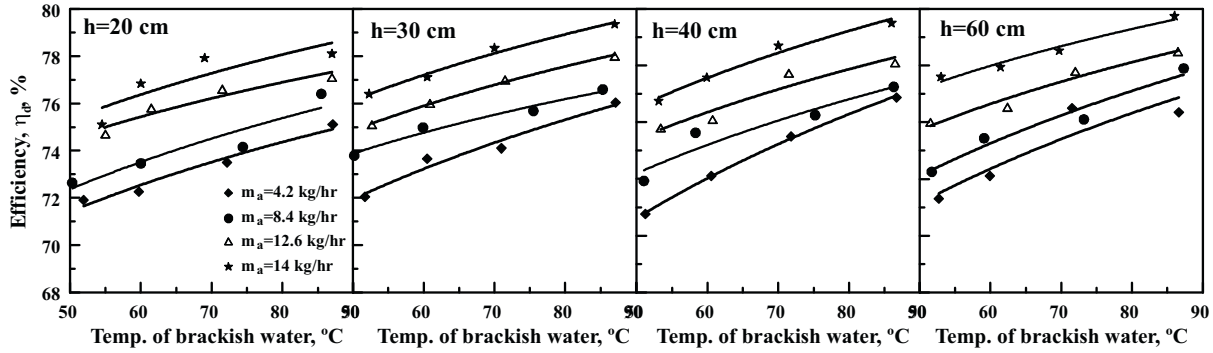

Fig. 7. The effect of the brackish water temperature on efficiency of the desalination at different airflow rates and brackish water levels.

Table 2
The value of productivity and the cost of productivity at different water temperatures and air flow rates.

$\dot{m}_a$ (kg/h)	T_w = 50 °C		T_w = 60 °C		T_w = 70 °C		T_w = 80 °C	
	$\dot{m}_w$ (kg/h)	CPL ($/kg$_w$)	$\dot{m}_w$ (kg/h)	CPL ($/kg$_w$)	$\dot{m}_w$ (kg/h)	CPL ($/kg$_w$)	$\dot{m}_w$ (kg/h)	CPL ($/kg$_w$)
4.20	0.39	0.08	0.88	0.046	1.52	0.046	2.64	0.072
8.40	0.63	0.08	1.41	0.046	2.73	0.056	4.88	0.079
12.60	0.83	0.08	1.77	0.057	3.02	0.061	5.20	0.114
14.00	0.85	0.08	1.79	0.059	3.39	0.066	5.93	0.115

8. Cost analysis

The better economic return on the investment depends on the production cost of the distilled water and its applicability. Fath et al. [23] give economical analysis of water desalination unit. The capital recovery factor (CRF), the fixed annual cost (FAC), the sinking fund factor (SFF), the annual salvage value (ASV), average annual productivity ($\dot{m}_w$), maintenance cost (AMC), current cost (CC) (0.06 $/kW h) and annual cost (AC) are the main calculation parameters used in the cost analysis of the desalination unit. Finally, the cost of distilled water per liter (CPL) can be calculated by dividing the net annualized cost of the system (AC) by annual yield of solar still (M). The above-mentioned calculation parameters can be expressed as [1]:

$$\mathrm{CRF} = \frac{i(1+i)^n}{(1+i)^n - 1} \tag{6}$$

$$\mathrm{FAC} = \mathrm{P(CRF)} \tag{7}$$

$$\mathrm{SFF} = \frac{i}{(1+i)^n - 1} \tag{8}$$

$$S = 0.2\mathrm{P} \tag{9}$$

$$\mathrm{AMC} = 0.15\mathrm{FAC} \tag{10}$$

$$\mathrm{ACC} = \mathrm{CC} \times \mathrm{Power} \tag{11}$$

$$\mathrm{AC} = \mathrm{FAC} + \mathrm{AMC} + \mathrm{ACC} - \mathrm{ASV} \tag{12}$$

$$\mathrm{CPL} = \frac{\mathrm{AC}}{\mathrm{M}} \tag{13}$$

where P: is the present capital cost of desalination system (700 $); i: is the interest per year, which is assumed as 12%; n: is the number of life years, which is assumed 10 years in this analysis. ACC: is the cost of power used in system.

Table 2 shows the value of productivity and the cost of productivity at different water temperatures and airflow rates. From table, as increase airflow rate from 4.2 to 14 kg/h the average cost of water production about 0.08 $/kg at 50 °C, 0.052 $/kg at 60 °C, 0.057 $/kg at 70 °C and 0.095 $/kg at 80 °C.

The high cost of fresh water shown in Table 2 is due to use high present capital cost of desalination system because high price of compressor and high interest per year and maintenance cost (AMC) is equal to .15 of the fixed annual cost. When this system applied commercially in large scale, the cost of fresh water will be decreased.

9. Conclusions

The experimental and theoretical investigation of the principal operating parameters of a desalination process working with an air humidification–dehumidification method is studied. The effects of the water temperature, water level and airflow rate on the humidification effectiveness, productivity and efficiency of the system were observed during the present experiments and the following points were concluded.

The productivity of the system increases with the increase of the water temperature and airflow rate. The productivity of the system is moderately affected by the water temperature and airflow rate while slightly affected by the water level. The humidification effectiveness and the efficiency of the desalination system are higher for $\dot{m}_a = 14$ kg/h at different water temperatures and levels. At 80 °C, the productivity of the system is higher at different water levels and airflow rates except $\dot{m}_a = 4.2$ kg/h. The experimental measured agreed well with experimental calculation productivity. Within the studied ranges, the productivity of the system reached to 8.22 kg_w/h at 86 °C for water and $\dot{m}_a = 14$ kg/h.

References

[1] M. Farid, S. A1-Hajaj, Solar desalination with a humidification–dehumidification cycle, Desalination 106 (1996) 427–429.
[2] S. Al-Hallaj, M.M. Farid, A.R. Tamimi, Solar desalination with a humidification–dehumidification cycle: performance of the unit, Desalination 120 (1998) 273–280.
[3] A.S. Nafey, H.E.S. Fath, S.O. El-Helaby, A.M. Soliman, Solar desalination using humidification–dehumidification processes. Part II. An experimental investigation, Energy Conversion and Management 45 (2004) 1263–1277.
[4] G. Al-Enezi, H. Ettouney, N. Fawzy, Low temperature humidification dehumidification desalination process, Energy Conversion and Management 47 (2006) 470–484.
[5] M. Ben-Amara, I. Houcine, A. Guizani, M. Mfialej, Experimental study of a multiple-effect humidification solar desalination technique, Desalination 170 (2004) 209–221.
[6] E. Chafik, A new seawater desalination process using solar energy, Desalination 153 (2002) 25–37.
[7] E. Chatik, A new type of seawater desalination plants using solar energy, Desalination 156 (2003) 333–348.
[8] H. Ettouney, Design and analysis of humidification dehumidification desalination process, Desalination 183 (2005) 341–352.
[9] M.M. Farid, S. Parekh, J.R. Selman, S. Al-Hallaj, Solar desalination with a humidification dehumidification cycle: mathematical modeling of the unit, Desalination 151 (2002) 153–164.
[10] A.S. Nafey, H.E.S. Fath, S.O. El-Helaby, A.M. Soliman, Solar desalination using humidification dehumidification processes. Part I. A numerical investigation, Energy Conversion and Management 45 (2004) 1243–1261.
[11] N.K. Nawayseh, M.M. Farid, A. Omar, A. Sabirin, Solar desalination based on humidification process – II. Computer simulation, Energy Conversion and Management 40 (1999) 1441–1461.
[12] J. Orfi, N. Galanisb, M. Laplanteb, Air humidification–dehumidification for a water desalination system using solar energy, Desalination 203 (2007) 471–481.
[13] R. Xiong, W.S. Shichang, Z. Wang, A mathematical model for a thermally coupled humidification–dehumidification desalination process, Desalination 196 (2006) 177–187.
[14] G. Yuan, H. Zhang, Mathematical modeling of a closed circulation solar desalination unit with humidification–dehumidification, Desalination 205 (2007) 156–162.
[15] M. Vlachogiannis, V. Bontozoglou, C. Georgalas, G. Litinas, Desalination by mechanical compression of humid air, Desalination 122 (1999) 35–42.
[16] H.M. Ettouney, H.T. El-Dessouky, Y. Al-Roumi, Analysis of mechanical vapor compression desalination process, International Journal of Energy Research 23 (1999) 431–451.
[17] Y.J. Dai, H.F. Zhang, Experimental investigation of a solar desalination unit with humidification and dehumidification, Desalination 130 (2000) 169–175.
[18] H.P. Garg, R.S. Adhikari, R. Kumar, Experimental design and computer simulation of multi-effect humidification (MEH)–dehumidification solar distillation, Desalination 153 (2002) 81–86.
[19] S.A. El-Agouz, M. Abugderah, Experimental analysis of humidification process by air passing through seawater, Energy Conversion and Management 49 (2008) 3698–3703.

[20] R.E. Sonntag, C. Borgnakke, C.J. Van Wylen, Fundamentals of Thermodynamics, John Wiley & Sons, Inc, New York, 2003.
[21] K. Srithar, A. Mani, Analysis of a single cover FRP flat plate collector for treating tannery effluent, Applied Thermal Engineering 24 (2004) 873–883.
[22] N.C. Barford, Experimental Measurements: Precision Error and Truth, John Wiley & Sons, New York, 1990.
[23] H.E.S. Fath, M. El-Samanoudy, K. Fahmy, A. Hassabou, Thermal-economic analysis and comparison between pyramid shaped and single-slope solar still configurations, Desalination 159 (2003) 69–79.